

# Relationship between epithelial organization and morphogen interpretation

**Review Article****Author(s):**

Iber, Dagmar ; Vetter, Roman 

**Publication date:**

2022-08

**Permanent link:**

<https://doi.org/10.3929/ethz-b-000550937>

**Rights / license:**

[Creative Commons Attribution-NonCommercial-NoDerivatives 4.0 International](#)

**Originally published in:**

Current Opinion in Genetics & Development 75, <https://doi.org/10.1016/j.gde.2022.101916>

# Relationship between epithelial organization and morphogen interpretation

Dagmar Iber<sup>1,2</sup> and Roman Vetter<sup>1,2</sup>



Despite molecular noise and genetic differences between individuals, developmental outcomes are remarkably constant. Decades of research has focused on the underlying mechanisms that ensure this precision and robustness. Recent quantifications of chemical gradients and epithelial cell shapes provide novel insights into the basis of precise development. In this review, we argue that these two aspects may be linked in epithelial morphogenesis.

## Addresses

<sup>1</sup> Department of Biosystems Science and Engineering, ETH Zürich, Mattenstrasse 26, 4058 Basel, Switzerland

<sup>2</sup> Swiss Institute of Bioinformatics, Mattenstrasse 26, 4058 Basel, Switzerland

Corresponding author: Dagmar Iber ([dagmar.iber@bsse.ethz.ch](mailto:dagmar.iber@bsse.ethz.ch))

Current Opinion in Genetics & Development 2022, 75:101916

This review comes from a themed issue on **Developmental mechanisms, patterning and evolution**

Edited by **Magali Suzanne** and **Miguel Torres Sanchez**

<https://doi.org/10.1016/j.gde.2022.101916>

0959-437X/© 2022 The Author(s). Published by Elsevier Ltd. This is an open access article under the CC-BY-NC-ND license (<http://creativecommons.org/licenses/by-nc-nd/4.0/>).

## Introduction

Epithelia are among the first tissue types to emerge during morphogenesis. A hallmark of epithelia is apical–basal polarity (Figure 1). Beneath the apical surface, tight junctions create a watertight seal, and control the paracellular passage of ions and solutes between epithelial cells, while preventing the mixing of apical and basal–lateral membranes. The adhesion belt and further adhesive junctions along the lateral side stabilize the cell–cell contacts. On the basal-most side, epithelia bind tightly to the basal lamina. The first epithelial structure, the blastula, is a hollow sphere made of a single epithelial cell layer. At later stages, multilayered epithelia emerge. As development progresses, the simple epithelial sheets, tubes, and vesicles grow and deform into the complex shapes characteristic of organs and adult

tissues. These morphogenetic changes are guided by a wide range of mechanisms that use chemical signals, mechanical constraints, and fluid-flow-induced shear stress. As animals develop from a single cell, cells must take on the correct fate at the right position and time to build a functional organism. Developmental outcomes are remarkably constant, despite environmental, inter-individual, and evolutionary changes that alter reaction time and patterning length scales [1–3], a phenomenon coined as canalization. How such developmental precision and robustness is achieved is still largely unknown. While mechanical contributions have recently received greater attention, precision of morphogenesis has, so far, mainly been studied for gradient-based patterning.

## Morphogen gradient precision

The measured morphogen gradients can be approximated well either by an exponential function

$$C(x) = C_0 e^{-x/\lambda} \quad (1)$$

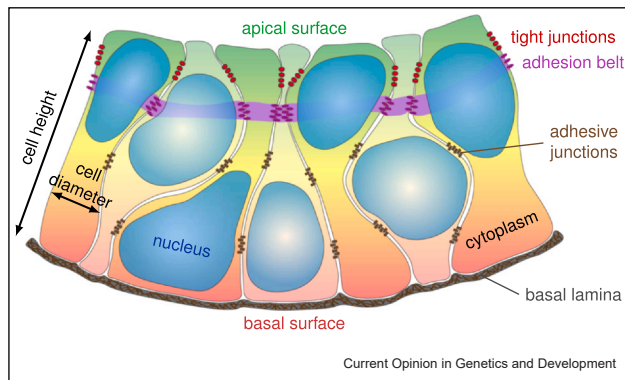
with an amplitude  $C_0$  at the morphogen source at  $x = 0$  and a decay length  $\lambda$  (Figure 2a), or by a power law

$$C(x) = A(x + x_0)^{-m}, \quad (2)$$

where  $A$ ,  $m$ ,  $x_0$  are positive constants [4–9]. These gradient profiles emerge independent of whether morphogen transport happens via diffusion or cytonemes [10]. Diffusion-based gradients have been argued to be more precise for large gradient length, and vice versa [11]. Power-law gradients arise from ligand-enhanced degradation and are less sensitive to a variable source [12], but the shallower gradient profile far away from the source limits their usefulness [13]. It has been argued that the best cost-precision trade-off can be achieved when gradients are read out at about  $2\lambda$  from the source [14], but patterning distances are much larger in the neural tube (NT) [7], and SHH-dependent responses are observed even in the very dorsal NT, which is more than  $10\lambda$  away from the SHH source [15].

According to the French flag model, morphogen gradients define different tissue domains via concentration thresholds (Figure 2a) [16,17], although intracellular regulatory networks can result in more complex dependencies [18,19]. In case of a threshold-based readout, cells exposed to morphogen concentrations above the threshold take on a different fate from cells exposed to lower concentrations. Measurements in several developmental systems reveal the direct readouts of the

Figure 1



Cell polarity in a pseudostratified epithelial layer.

morphogen gradients to be smooth [7,20,17,21]. Sharp transitions require ultrasensitive readout mechanisms, which may include features such as cooperativity, zero-order ultrasensitivity, or hysteresis, among others. Bistable networks have been explored to explain sharp boundaries in development, and to engineer gradient-based patterning in synthetic biology approaches [21–26]. Also with sharp readouts, noise can still result in a transition zone with mixed cell fates (Figure 2b), resulting in misaligned boundaries in morphogenetic fields of single embryos. As the morphogen concentration declines with distance from the source, noise-driven transition zones have been suggested to widen [13]. Cell alignment along sharp boundaries can be achieved via polarized contractility, adhesion-based cell sorting, and cell competition [27–32].

Deviations in the readout position,  $x_{\theta}$ , between embryos,  $i$ , are referred to as positional error (Figure 2c)

$$\sigma_x = \text{SD}\{x_{\theta,i}\}. \quad (3)$$

The positional error has been reported to be smaller for the readout than for the gradient [4,33,34,7], resulting in a quest for precision-enhancing mechanisms. Spatial and temporal averaging have been proposed to enhance precision in the *Drosophila* blastoderm syncytium [4], and the downstream-gap gene network has been suggested to act as an optimal decoder of upstream positional information by integrating maternal inputs across the embryo [35,36]. Similarly, optimal decoding of the opposing SHH and BMP gradients has been proposed to explain the high precision of the progenitor-domain boundaries in the center of the mouse NT [7]. However, the gradient variability had been overestimated, and single gradients would be precise enough to pattern the center [37].

Recent work highlights the importance of dynamics for patterning precision in the *Drosophila* blastoderm.

Precise patterning can be achieved faster when cellular decision times vary, depending on the statistical realization of the noisy signal, as formulated in Wald's sequential probability-ratio test [38], and the transient dynamics that emerge from the complex regulatory interactions in the gap gene network play an important role in patterning precision and canalization [19].

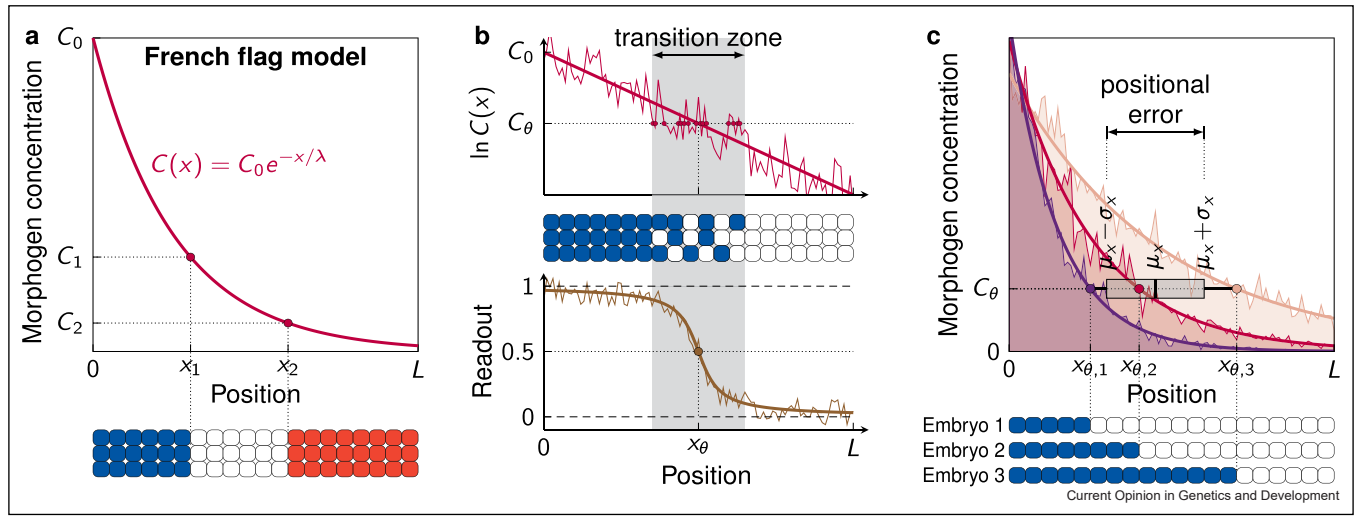
As concentration gradients spanning orders of magnitude are more difficult to image in their entirety than their sigmoidal readouts (Figure 2b), the possibility remains that the reported higher gradient variability reflects technical errors. For the reported molecular noise levels in morphogen production, decay, and transport, cell-based simulations predict a gradient variability that is consistent with the observed precision of readouts, even at very large distances from the source [37,39]. Morphogen gradients may thus be more precise than thought and provide sufficient positional information on their own.

### Relationship between cellular organization and patterning precision

Large cell diameters in the patterning direction increase gradient variability via their impact on morphogen production, removal, and transport, while spatial averaging over the cell surface or via cilia- or cytoneme-based sensing has only a small impact in the cell-based simulations (Figure 3a). Here, it is only important to limit the cell diameter in patterning direction, but not necessarily in the orthogonal directions. Interestingly, in the developing lung, where no gradient-based patterning has been described, the apical surfaces are elongated in the direction of preferential outgrowth [41], while in the NT, where gradients pattern the tissue along the axis of preferential outgrowth, this is not the case [42,43]. Many ligands are sensed also on the basal-lateral side [44,45], but the same principles that apply apically also apply basal-laterally: also in this case, smaller cell diameters in the patterning direction will result in less variability. As morphogens must diffuse through the intercellular space to reach the lateral sides, the effective diffusion path is, however, longer than the beeline [46]. This phenomenon is commonly referred to as tortuosity, and alters the effective macroscopic morphogen diffusivity.

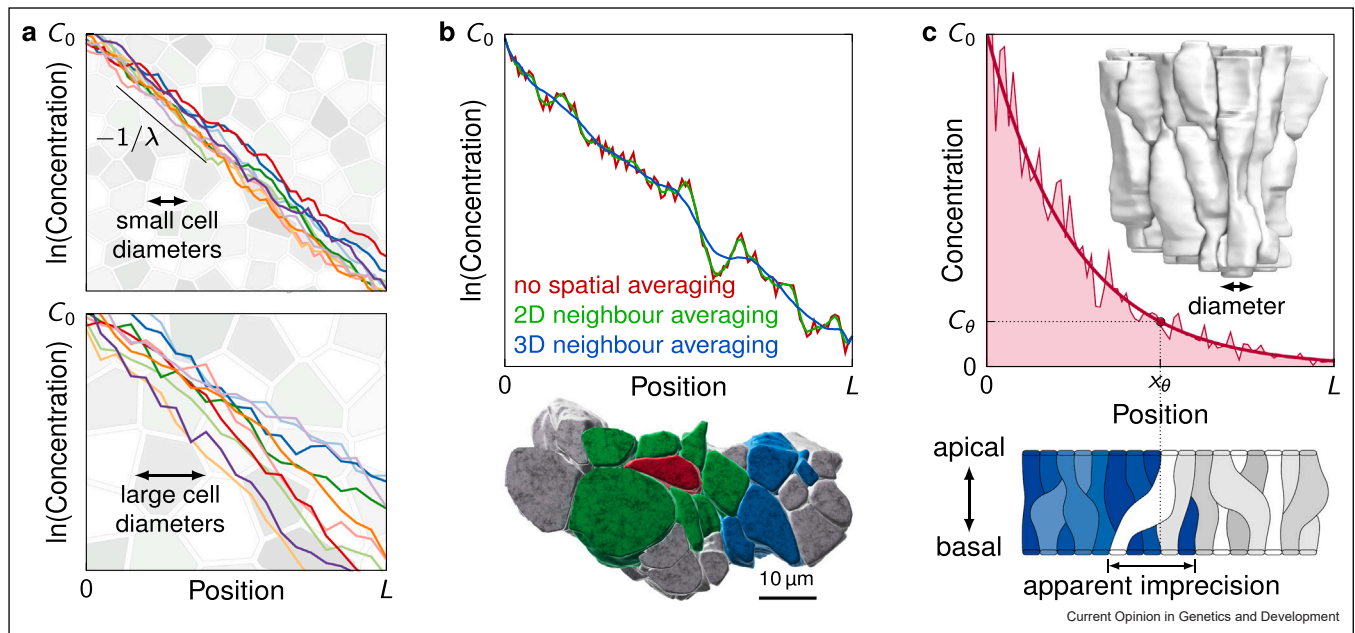
The apical surfaces are small in all epithelia that are known to employ gradient-based patterning and that have been quantified [39]. A small apical surface is not necessarily a reflection of small overall cell size, as measured by its volume. For one, tissue curvature can result in smaller apical surfaces (Figure 1a). In the NT, the SHH-sensing cilium is indeed located on the inner, apical surface [47], while in the flat *Drosophila* wing and eye discs, cells sense Hh along the entire apical-basal axis [45]. Finally, several morphogens, including SHH

Figure 2



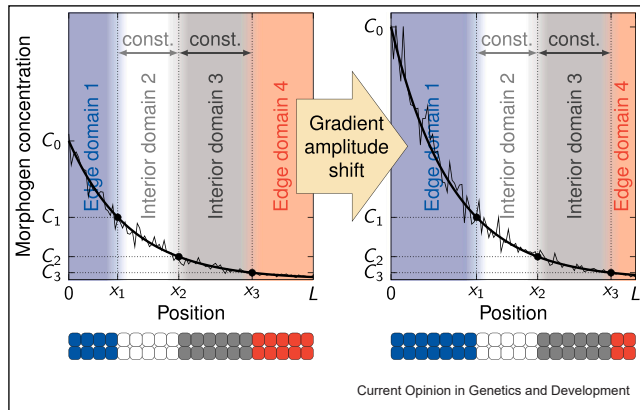
Morphogen gradient precision. **(a)** The French flag model and the French flag patterning problem. **(b)** Transition zones are not necessarily sharp. The noisy gradient reaches the readout threshold  $C(x) = C_\theta$  at several positions (purple dots). The readout position  $x_\theta$  (brown dot) is set as the position where the averaged morphogen concentration (pink line) equals the Hill constant of the sigmoidal readout (brown line); alternative definitions exist. **(c)** Variability in the gradients translates into different readout positions.  $\mu_x$  is the mean readout position of the three gradients.

Figure 3



Relationship between cellular organization and patterning precision. **(a)** Morphogen gradients across tissues with small cell diameters are less variable than with large cell diameters. **(b)** Spatial concentration averaging over cell neighborhoods reduces gradient variability only little; long-range 3D cell contacts may increase this effect. Colors as below in the epithelium. Bottom: Nonlocal cell neighborhood in the mouse lung epithelium as seen on the apical surface, reproduced with modifications from Ref. [40]. Green and blue cells are in direct contact with the red cell somewhere along the apical-basal axis, even though on the surface, only green neighbors are apparent. **(c)** The complex noncolumnar shape of cells in pseudostratified epithelia may give rise to an apparent imprecision of domain boundaries (blue/white). Inset: Epithelial cells in the monolayer epithelium of the developing mouse lung. Dataset from Ref. [40]. All noisy gradients are artificially created for illustration.

Figure 4



Precision of progenitor cell numbers. In interior patterning domains (white, gray), cell numbers (bottom) are preserved under changes in the amplitude  $C_0$  of exponential morphogen gradients.

and ligands of the TGF- $\beta$  and the WNT family, have been shown to increase the apical–basal height of epithelial cells, and thus shrink the cell diameter, via their impact on actin polymerization, myosin localization, and activity [48–50]. Morphogen signaling itself may thus result in small epithelial cell diameters — a relationship that deserves further clarification.

For narrow cells, the nucleus — albeit deformable — is wider than the average cell diameter (Figure 1), and the nuclei disperse along the apical–basal axis, a phenomenon commonly referred to as pseudostratification [40,51]. During mitosis, the nuclei must locate to the apical surface. As there is insufficient space to accommodate all nuclei apically, they move toward the basal side during the G1 phase, and back to the apical surface during the G2 phase in a process termed interkinetic nuclear migration (IKNM) [51]. The evolutionary driving force behind the emergence of pseudostratification has so far remained elusive, but may now be explicable with the importance of slim cells for high patterning precision.

Cells in pseudostratified epithelia change their neighbor relationships several times along the apical–basal axis in an effort to minimize the surface area that covers their complex cell shapes [40]. They are thus in contact with many more cells than what is apparent on the apical or basal cell surface (Figure 3b), and potentially sense ligands over a wider distance. The neighbor relationships change dynamically over time, facilitating the sorting of epithelial cells to create sharper boundaries [32,40].

Going forward, it will be important to analyze expression domain boundaries in 3D. Cells or nuclei that may appear as if they were in the ‘wrong’ position in 2D slices

may actually be in the correct domain (Figure 3c). Given the fluidity of cell contacts, establishing sharp boundaries may not be as relevant as producing cells of a certain type in correct numbers, as determined by the size of individual domains. The size of interior domains is more precise than the position of their domain boundaries if the gradient shape remains exponential because changes in the gradient amplitude shift the position of the domain without altering its size (Figure 4) [37].

## Conclusion and outlook

Patterning precision has long been analyzed with a focus on the information content of chemical gradients. It is becoming increasingly evident that tissues achieve high patterning precision not only by minimizing molecular noise in chemical reactions, but also by controlling cell and tissue geometry [2,39]. Mechanical stress patterns that depend on the cellular contractility and substrate stiffness may also contribute to tissue patterning [52]. Finally, tissue patterning and growth are intricately linked. Morphogens control not only patterning, cell differentiation, and cell shapes, but also the tissue growth rate [6]. How embryos control tissue size and how patterns scale with domain size remains a field of intense inquiry (e.g. [9,53–57]). Synthetic gradients [58,53,59] and computational frameworks that enable high-resolution 3D cell-based tissue simulations [60] are promising tools to understand how nature achieves robust and reliable patterning to an extent that the same molecular patterning mechanism can be reused in evolution, despite large changes in tissue size and developmental rate.

## Conflict of interest statement

Nothing declared.

## Acknowledgements

This work was funded by Swiss National Science Foundation (SNF) Sinergia Grant CRSII5 70930. We thank Kevin Yamauchi for helpful comments, and apologize to those authors whose work we could not discuss due to length and citation constraints.

## References and recommended reading

Papers of particular interest, published within the period of review, have been highlighted as:

- of special interest
  - of outstanding interest
1. Zhu H, Cui Y, Luo C, Liu F: **Quantifying temperature compensation of bicoid gradients with a fast t-tunable microfluidic device.** *Biophys J* 2020, **119**:1193–1203, <https://doi.org/10.1016/j.bpj.2020.08.003>
  2. Huang A, Rupprecht JF, Saunders TE: **Embryonic geometry underlies phenotypic variation in decanalized conditions.** *eLife* 2020, **9**:e47380, <https://doi.org/10.7554/eLife.47380>. Tissue geometry plays an important role in buffering perturbations in morphogen dosage: a rounder *Drosophila* egg shape renders the embryo more sensitive to changes in *bicoid* dosage.
  3. Rayon T, Briscoe J: **Cross-species comparisons and in vitro models to study tempo in development and homeostasis.**

- Interface Focus* 2021, **11**:20200069, <https://doi.org/10.1098/rsfs.2020.0069>
4. Gregor T, Tank DW, Wieschaus EF, Bialek W: **Probing the limits to positional information.** *Cell* 2007, **130**:153-164, <https://doi.org/10.1016/j.cell.2007.05.025>
  5. Wartlick O, Kicheva A, González-Gaitán M: **Morphogen gradient formation.** *Cold Spring Harb Perspect Biol* 2009, **1**:a001255, <https://doi.org/10.1101/cshperspect.a001255>
  6. Wartlick O, Mumcu P, Kicheva A, Bittig T, Seum C, Jülicher F, González-Gaitán M: **Dynamics of Dpp signaling and proliferation control.** *Science* 2011, **331**:1154-1159, <https://doi.org/10.1126/science.1200037>
  7. Zagorski M, Tabata Y, Brandenberg N, Lutolf MP, Tkacik G, Bollenbach T, Briscoe J, Kicheva A: **Decoding of position in the developing neural tube from antiparallel morphogen gradients.** *Science* 2017, **356**:1379-1383, <https://doi.org/10.1126/science.aam5887>
  8. Chan WK, Price DJ, Pratt T: **FGF8 morphogen gradients are differentially regulated by heparan sulphotransferases Hs2st and Hs6st1 in the developing brain.** *Biol Open* 2017, **6**:1933-1942, <https://doi.org/10.1242/bio.028605>
  9. Mateus R, Holtzer L, Seum C, Hadjivasiliou Z, Dubois M, Jülicher F, González-Gaitán M: **BMP signaling gradient scaling in the Zebrafish Pectoral Fin.** *Cell Rep* 2020, **30**:4292-4302, <https://doi.org/10.1016/j.celrep.2020.03.024>
  10. Aguirre-Tamaral A, Guerrero I: **Improving the understanding of cytoneme-mediated morphogen gradients by in silico modeling.** *PLoS Comput Biol* 2021, **17**:1-30, <https://doi.org/10.1371/journal.pcbi.1009245>
  11. Fancher S, Mugler A: **Diffusion vs. direct transport in the precision of morphogen readout.** *eLife* 2020, **9**:e58981, <https://doi.org/10.7554/eLife.58981>.  
Theoretical considerations suggest that for large gradient length, diffusion-based gradients are more precise than those created by direct transport, and vice versa.
  12. Eldar A, Rosin D, Shilo B-Z, Barkai N: **Self-enhanced ligand degradation underlies robustness of morphogen gradients.** *Dev Cell* 2003, **5**:635-646, [https://doi.org/10.1016/S1534-5807\(03\)00292-2](https://doi.org/10.1016/S1534-5807(03)00292-2)
  13. Lander AD, Lo W-C, Nie Q, Wan FYM: **The measure of success: constraints, objectives, and tradeoffs in morphogen-mediated patterning.** *CSH Perspect Biol* 2009, **1**:a002022, <https://doi.org/10.1101/cshperspect.a002022>
  14. Song Y, Hyeon C: **Cost-precision trade-off relation determines the optimal morphogen gradient for accurate biological pattern formation.** *eLife* 2021, **10**:e70034, <https://doi.org/10.7554/eLife.70034>
  15. Oostervert T, Kurdija S, Enstero M, Uhde CW, Bergsland M, Sandberg M, Sandberg R, Muhr J, Ericson J: **SoxB1-driven transcriptional network underlies neural-specific interpretation of morphogen signals.** *Proc Natl Acad Sci USA* 2013, **110**:7330-7335, <https://doi.org/10.1073/pnas.1220010110>
  16. Wolpert L: **Positional information and the spatial pattern of cellular differentiation.** *J Theor Biol* 1969, **25**:1-47, [https://doi.org/10.1016/S0022-5193\(69\)80016-0](https://doi.org/10.1016/S0022-5193(69)80016-0)
  17. Greenfeld H, Lin J, Mullins MC: **The BMP signaling gradient is interpreted through concentration thresholds in dorsal-ventral axial patterning.** *PLoS Biol* 2021, **19**:e3001059, <https://doi.org/10.1371/journal.pbio.3001059>.  
By combining modelling and quantitative measurements, the authors provide evidence in favour of a threshold-based interpretation of the BMP gradient in the zebrafish dorsal-ventral axis.
  18. Rogers KW, ElGamacy M, Jordan BM, Muller P: **Optogenetic investigation of bmp target gene expression diversity.** *eLife* 2020, **9**:e58641, <https://doi.org/10.7554/eLife.58641>.  
The cellular response to optogenetically delivered high and low amplitude signals show that the readout of the BMP gradient along the zebrafish dorsal-ventral axis is not entirely threshold-based. Transcriptional kinetics and combinatorial signalling further shape the response.
  19. Jaeger J, Verd B: **Dynamic positional information: patterning mechanism versus precision in gradient-driven systems.** *Curr Top Dev Biol* 2020, **137**:219-246, <https://doi.org/10.1016/bs.ctdb.2019.11.017>
  20. Bakker R, Mani M, Carthew RW: **The Wg and Dpp morphogens regulate gene expression by modulating the frequency of transcriptional bursts.** *eLife* 2020, **9**:e56076, <https://doi.org/10.7554/eLife.56076>.  
Using single molecule fluorescence *in situ* hybridization, the authors find that the Dpp and Wg morphogen gradients modulate the frequency of transcriptional bursts. The mRNA profiles of direct readouts are smooth.
  21. Guillaume G, de Buyl S, Sirour C, Haupaix N, Bettoni R, Imai KS, Satou Y, Dupont G, Hudson C, Yasuo H: **Cell geometry, signal dampening, and a bimodal transcriptional response underlie the spatial precision of an ERK-mediated embryonic induction.** *Dev Cell* 2021, **56**:2966-2979, <https://doi.org/10.1016/j.devcel.2021.09.025>.  
Ascidia combine a smooth interpretation of the FGF gradient and signal dampening via ephrin to achieve precise induction of neural cell fate in two out of eight ectodermal cells.
  22. Balaskas N, Ribeiro A, Panovska J, Dessaud E, Sasai N, Page KM, Briscoe J, Ribes V: **Gene regulatory logic for reading the Sonic Hedgehog signaling gradient in the vertebrate neural tube.** *Cell* 2012, **148**:273-284, <https://doi.org/10.1016/j.cell.2011.10.047>
  23. Grant PK, Szep G, Patange O, Halatek J, Coppard V, Csikasz-Nagy A, Haseloff J, Locke JCW, Dalchau N, Phillips A: **Interpretation of morphogen gradients by a synthetic bistable circuit.** *Nat Commun* 2020, **11**:5545, <https://doi.org/10.1038/s41467-020-19098-w>
  24. Barbier I, Perez-Carrasco R, Schaerli Y: **Controlling spatiotemporal pattern formation in a concentration gradient with a synthetic toggle switch.** *Mol Syst Biol* 2020, **16**:e9361, <https://doi.org/10.15252/msb.20199361>
  25. Exelby K, Herrera-Delgado E, Garcia Perez L, Perez-Carrasco R, Sagner A, Metzis V, Sollich P, Briscoe J: **Precision of tissue patterning is controlled by dynamical properties of gene regulatory networks.** *Development* 2021, **148**:dev197566, <https://doi.org/10.1242/dev.197566>
  26. Perkins ML: **Implications of diffusion and time-varying morphogen gradients for the dynamic positioning and precision of bistable gene expression boundaries.** *PLoS Comput Biol* 2021, **17**:1-25, <https://doi.org/10.1371/journal.pcbi.1008589>
  27. Xiong F, Tentner AR, Huang P, Gelas A, Mosaliganti KR, Souhait L, Rannou N, Swinburne IA, Obholzer ND, Cowgill PD, Schier AF, Megason SG: **Specified neural progenitors sort to form sharp domains after noisy Shh signaling.** *Cell* 2013, **153**:550-561, <https://doi.org/10.1016/j.cell.2013.03.023>
  28. Akieda Y, Ogami S, Furuie H, Ishitani S, Akiyoshi R, Nogami J, Masuda T, Shimizu N, Ohkawa Y, Ishitani T: **Cell competition corrects noisy Wnt morphogen gradients to achieve robust patterning in the zebrafish embryo.** *Nat Commun* 2019, **10**:4710, <https://doi.org/10.1038/s41467-019-12609-4>
  29. Tsai TY-C, Sikora M, Xia P, Colak-Champollion T, Knaut H, Heisenberg C-P, Megason SG: **An adhesion code ensures robust pattern formation during tissue morphogenesis.** *Science* 2020, **370**:113-116, <https://doi.org/10.1126/science.aba6637>.  
By measuring adhesion forces and the combinatorial expression of different cadherins by neural progenitors, the authors show that the SHH gradient in the zebrafish NT sets up a differential adhesion code that enables the emergence of sharp boundaries.
  30. Eritano AS, Bromley CL, BoleaAlbero A, Schutz L, Wen FL, Takeda M, Fukaya T, Sami MM, Shibata T, Lemke S, Wang YC: **Tissue-scale mechanical coupling reduces morphogenetic noise to ensure precision during epithelial folding.** *Dev Cell* 2020, **53**:212-228, <https://doi.org/10.1016/j.devcel.2020.02.012>.  
Polarised, mechanical coupling ensures precision during epithelial folding even though cellular noise in motor non-muscle myosin II levels prevents the precise translation of the positional information of the morphogen gradient into a precise cellular response.
  31. Martin E, Theis S, Gay G, Monier B, Rouvière C, Suzanne M: **Mechanical control of morphogenetic robustness in an**

- inherently challenging environment.** *BioRxiv* 2021,, <https://doi.org/10.1101/2020.01.06.896266>
32. Bocanegra-Moreno L, Singh A, Hannezo E, Zagorski M, Kicheva A: **Cell cycle dynamics controls fluidity of the developing mouse neuroepithelium.** *BioRxiv* 2022,, <https://doi.org/10.1101/2022.01.20.477048>
  33. He F, Wen Y, Deng J, Lin X, Lu LJ, Jiao R, Ma J: **Probing intrinsic properties of a robust morphogen gradient in Drosophila.** *Dev Cell* 2008, **15**:558-567, <https://doi.org/10.1016/j.devcel.2008.09.004>
  34. Bollenbach T, Pantazis P, Kicheva A, Bökel C, González-Gaitán M, Jülicher F: **Precision of the Dpp gradient.** *Development* 2008, **135**:1137-1146, <https://doi.org/10.1242/dev.012062>
  35. Petkova MD, Tkacik G, Bialek W, Wieschaus EF, Gregor T: **Optimal decoding of cellular identities in a genetic network.** *Cell* 2019, **176**:844-855, <https://doi.org/10.1016/j.cell.2019.01.007>
  36. Tkacik G, Gregor T: **The many bits of positional information.** *Development* 2021, **148**:dev176065, <https://doi.org/10.1242/dev.176065>
  37. Vetter R, Iber D: **Precision of morphogen gradients in neural tube development.** *Nat Commun* 2022, **13**:1145, <https://doi.org/10.1038/s41467-022-28834-3>
  38. Desponds J, Vergassola M, Walczak AM: **A mechanism for hunchback promoters to readout morphogenetic positional information in less than a minute.** *eLife* 2020, **9**:e49758, <https://doi.org/10.7554/eLife.49758>.  
Fast, precise morphogen readouts can be achieved if cells employ Wald's Sequential Probability Ratio Test, and the cellular decision time depends on the statistical realisation of the noisy signal.
  39. Adelman JA, Vetter R, Iber D: **Impact of cell size on morphogen gradient precision.** *BioRxiv* 2022,, <https://doi.org/10.1101/2022.02.02.478800>
  40. Gómez HF, Dumond MS, Hodel L, Vetter R, Iber D: **3D cell neighbour dynamics in growing pseudostratified epithelia.** *eLife* 2021, **10**:e68135, <https://doi.org/10.7554/eLife.68135>.  
Provides the first 3D segmentation of cells in pseudostratified epithelia, and reveals many more neighbour changes along the apical-basal axis than previously expected. 3D cell packing is explained with the minimisation of lateral cell-cell contact energy, for the given area variability. Neighbour changes are predominantly created by nuclei that undergo IKNM.
  41. Tang N, Marshall WF, McMahon M, Metzger RJ, Martin GR: **Control of mitotic spindle angle by the ras-regulated erk1/2 pathway determines lung tube shape.** *Science* 2011, **333**:342-345, <https://doi.org/10.1126/science.1204831>
  42. Kicheva A, Bollenbach T, Ribeiro A, Pérez Valle H, Lovell-Badge R, Episkopou V, Briscoe J: **Coordination of progenitor specification and growth in mouse and chick spinal cord.** *Science* 2014, **345**:1254927, <https://doi.org/10.1126/science.1254927>
  43. Guerrero P, Perez-Carrasco R, Zagorski M, Page D, Kicheva A, Briscoe J, Page KM: **Neuronal differentiation influences progenitor arrangement in the vertebrate neuroepithelium.** *Development* 2019, **146**:dev176297, <https://doi.org/10.1242/dev.176297>
  44. Zhang Z, Zwick S, Loew E, Grimley JS, Ramanathan S: **Mouse embryo geometry drives formation of robust signaling gradients through receptor localization.** *Nat Commun* 2019, **10**:4516, <https://doi.org/10.1038/s41467-019-12533-7>
  45. Gore T, Matussek Ta, D'Angelo G, Giordano C, Tognacci T, Lavenant-Staccini L, Rabouille C, Théron PP: **The GTPase Rab8 differentially controls the long- and short-range activity of the Hedgehog morphogen gradient by regulating Hedgehog apico-basal distribution.** *Development* 2021, **148**:dev191791, <https://doi.org/10.1242/dev.191791>.  
By analysing the role of the GTPase Rab8, the authors show that the apical and basolateral secretion of Hh differentially affects short-range and long-range targets.
  46. Muller P, Rogers KW, Yu SR, Brand M, Schier AF: **Morphogen transport.** *Development* 2013, **140**:1621-1638, <https://doi.org/10.1242/dev.083519>
  47. Saade M, Gutierrez-Vallejo I, Le Dreau G, Rabadan MA, Miguez DG, Buceta J, Marti E: **Sonic hedgehog signaling switches the mode of division in the developing nervous system.** *Cell Rep* 2013, **4**:492-503, <https://doi.org/10.1016/j.celrep.2013.06.038>
  48. Gritti-Linde A, Bei M, Maas R, Zhang XM, Linde A, McMahon AP: **Shh signaling within the dental epithelium is necessary for cell proliferation, growth and polarization.** *Development* 2002, **129**:5323-5337, <https://doi.org/10.1242/dev.00100>
  49. Legoff L, Rouault H, Lecuit T: **A global pattern of mechanical stress polarizes cell divisions and cell shape in the growing Drosophila wing disc.** *Development* 2013, **140**:4051-4059, <https://doi.org/10.1242/dev.090878>
  50. Kadzik RS, Cohen ED, Morley MP, Stewart KM, Lu MM, Morrisey EE: **Wnt ligand/Frizzled 2 receptor signaling regulates tube shape and branch-point formation in the lung through control of epithelial cell shape.** *Proc Natl Acad Sci USA* 2014, **111**:12444-12449, <https://doi.org/10.1073/pnas.1406639111>
  51. Norden C: **Pseudostratified epithelia — cell biology, diversity and roles in organ formation at a glance.** *J Cell Sci* 2017, **130**:1859-1863, <https://doi.org/10.1242/jcs.192997>
  52. Nunley H, Xue X, Fu J, Lubensky DK: **Generation of fate patterns via intercellular forces.** *BioRxiv* 2021,, <https://doi.org/10.1101/2021.04.30.442205>
  53. Stapornwongkul KS, de Gennes M, Cocconi L, Salbreux G, Vincent J-P: **Patterning and growth control in vivo by an engineered GFP gradient.** *Science* 2020, **370**:321-327, <https://doi.org/10.1126/science.abb8205>
  54. Shen J, Liu F, Tang C: **Scaling dictates the decoder structure.** *BioRxiv* 2021,, <https://doi.org/10.1101/2021.03.04.433820>
  55. Zecca M, Struhl G: **A unified mechanism for the control of Drosophila wing growth by the morphogens Decapentaplegic and wingless.** *PLoS Biol* 2021, **19**:e3001111, <https://doi.org/10.1371/journal.pbio.3001111>
  56. Matsuda S, Schaefer JV, Mii Y, Hori Y, Bieli D, Taira M, Plückthun A, Afolter M: **Asymmetric requirement of Dpp/BMP morphogen dispersal in the Drosophila wing disc.** *Nat Commun* 2021, **12**:6435, <https://doi.org/10.1038/s41467-021-26726-6>
  57. Romanova-Michaelides M, Hadjivasilou Z, Aguilar-Hidalgo D, Basagiannis D, Seum C, Dubois M, Jülicher F, González-Gaitán M: **Morphogen gradient scaling by recycling of intracellular Dpp.** *Nature* 2022, **602**:287-293, <https://doi.org/10.1038/s41586-021-04346-w>
  58. Toda S, McKeithan WL, Hakkinen TJ, Lopez P, Klein OD, Lim WA: **Engineering synthetic morphogen systems that can program multicellular patterning.** *Science* 2020, **370**:327-331, <https://doi.org/10.1126/science.abc0033>
  59. Dupin A, Aufinger L, Styazhkin I, Rothfischer F, Kaufmann B, Schwarz S, Galensowske N, Clausen-Schaumann H, Simmel FC: **Synthetic cell-based materials extract positional information from morphogen gradients.** *Sci Adv* 2022, **8**:eabl9228, <https://doi.org/10.1126/sciadv.abl9228>
  60. Van Liedekerke P, Neitsch J, Johann T, Warmt E, Gonzalez-Valverde I, Hoehme S, Grosser S, Kaes J, Drasdo D: **A quantitative high-resolution computational mechanics cell model for growing and regenerating tissues.** *Biomech Model Mechanobiol* 2020, **19**:189-220, <https://doi.org/10.1007/s10237-019-01204-7>.  
Presents the first high-resolution 3D simulation framework with individually resolved, deformable, proliferating cells that can adhere to each other, or detach and migrate. While applied to spheroids and to regeneration in a liver lobule, the framework could potentially also be used to simulate the complex 3D epithelial cell dynamics.